High-Resolution Satellite Mapping of Fine Particulates Based on Geographically Weighted Regression

Bin Zou, Qiang Pu, Muhammad Bilal, Qihao Weng, Liang Zhai, and Janet E. Nichol

***Abstract*—Satellite-retrieved aerosol optical depth (AOD) has been increasingly utilized for the mapping of fine particulate matter ($PM_{2.5}$) concentrations. An accurate estimation and mapping of $PM_{2.5}$ concentrations depends on the high-resolution AOD data and a robust mathematical model that takes into account the spatial nonstationary relationship between $PM_{2.5}$ and AOD. Take the core portion of the Beijing–Hebei–Tianjin (Jing-Jin-Ji) urban agglomeration as case study (the most seriously polluted region in China). Land use, population, meteorological variables, and simplified aerosol retrieval algorithm-retrieved AOD at 1-km resolution are employed as the predictors for the geographically weighted regression (GWR) and the ordinary least squares (OLS) model to map the spatial distribution of $PM_{2.5}$ concentrations. The GWR model shows significant spatial variations in $PM_{2.5}$ concentrations over the region than the traditional OLS model, which reveals relative homogeneous variations. Validation with ground-level $PM_{2.5}$ concentrations demonstrates that $PM_{2.5}$ concentrations predicted by the GWR model ($R^2 = 0.75$, $RMSE = 10$ μg/m^3) correlate better than those by the OLS model ($R^2 = 0.53$, $RMSE = 16$ μg/m^3). These results suggest that the GWR model offered a more reliable way for the prediction of spatial distribution of $PM_{2.5}$ concentrations over urban areas.**

***Index Terms*—Aerosol optical depth (AOD), geographically weighted regression (GWR), moderate resolution imaging spectroradiometer (MODIS), $PM_{2.5}$, simplified aerosol retrieval algorithm (SARA), urban area.**

I. Introduction

FINE particulate matters with aerodynamic diameters less than 2.5 μm ($PM_{2.5}$) are of great concern to both the government and public due to their significant associations with increased cardiovascular and respiratory morbidity [1]. The adverse health effects of $PM_{2.5}$ pollution are more serious in China, the world-leading developing and the most heavily polluted country. Regular measurements of ground-level $PM_{2.5}$ concentrations are thus important for effectively alleviating public health concerns. While stationary ambient monitoring sites can provide real-time accurate $PM_{2.5}$ concentrations with high temporal resolution, the spatial resolution usually suffers from the sites' sparse distribution [2], [3]. Relatively, remote sensing provides a new way to estimate $PM_{2.5}$ concentration at an extensive spatial coverage by using satellite-derived aerosol optical depth (AOD) [4]–[6].

Previous studies examined the relationship between satellite-derived AOD and $PM_{2.5}$, which can be roughly divided into stages such as AOD retrieval and mathematical modeling. So far, spatial resolutions of AODs retrieved from the Moderate Resolution Imaging Spectroradiometer (MODIS), the Multiangle Imaging Spectroradiometer, and the Geostationary Operational Environmental Satellite Aerosol/Smoke Product [7], [8] generally range from 500 m to 17.6 km. AOD-based mathematical models mainly include linear regression models, artificial neural network algorithms, and chemical transport models [2]. In this process, the spatially non-stationary relationship between AOD and $PM_{2.5}$ has been recognized as essential to refine the $PM_{2.5}$ variations over urban area [5]. While researchers have growingly addressed the spatial nonstationarity by using geographically weighted regression (GWR) modeling in the recent three years [5], [9], [10], these studies are still improvable due to the usage of AOD with spatial resolution at 10 km. Because AOD at rough spatial resolution might reduce the performance, the GWR models cannot accurately reflect the local variations of $PM_{2.5}$ concentrations.

Therefore, the aim of this letter is to investigate the combination feasibility of high spatial resolution AOD and GWR modeling in adequately revealing the $PM_{2.5}$ variations at the local scale. To implement this goal, first, AOD is retrieved at 1-km spatial resolution from MODIS images for Jing-Jin-Ji urban agglomeration using a simplified aerosol retrieval algorithm (SARA). Thereafter, the quantitative local relationship between SARA AOD and $PM_{2.5}$ is built using GWR modeling technique with auxiliary parameters (i.e., land use, population, and meteorological variables).

II. Study Area and Data

A. Study Area

This letter focuses on the core portion of the Jing-Jin-Ji urban agglomeration (one of the largest metropolitan areas in China)

Manuscript received July 10, 2015; revised November 4, 2015 and January 5, 2016; accepted January 18, 2016. Date of publication February 29, 2016; date of current version March 23, 2016. This work was supported in part by the National Natural Science Foundation of China under Grant 41201384, by the Open Fund of University Innovation Platform, Hunan under Grant 15K132, by the National Geographic Conditions Monitoring under Grant HNGQJC2015-02, 2015JC03, the Key Laboratory for National Geographic Census and Monitoring, National Administration of Surveying, Mapping and Geoinformation under Grant 2014NGCM01, and by grants from the State Key Laboratory of Resources and Environmental Information System.

B. Zou and Q. Pu are with the School of Geosciences and Info-Physics, Central South University, Changsha 410078, China (e-mail: 210010@csu.edu.cn).

M. Bilal and J. E. Nichol are with the Department of Land Surveying and Geo-Informatics, Hong Kong Polytechnic University, Kowloon, Hong Kong (e-mail: muhammad.bilal@connect.polyu.hk).

Q. H. Weng is with the Center for Urban and Environmental Change, Indiana State University, Terre Haute, IN 47809 USA (e-mail: qweng@indstate.edu).

L. Zhai is with the Key Laboratory of Geo-Informatics of State Bureau of Surveying and Mapping, Chinese Academy of Surveying and Mapping, Beijing 100039, China (e-mail: zhailiang@casm.ac.cn).

Color versions of one or more of the figures in this paper are available online at http://ieeexplore.ieee.org.

Digital Object Identifier 10.1109/LGRS.2016.2520480

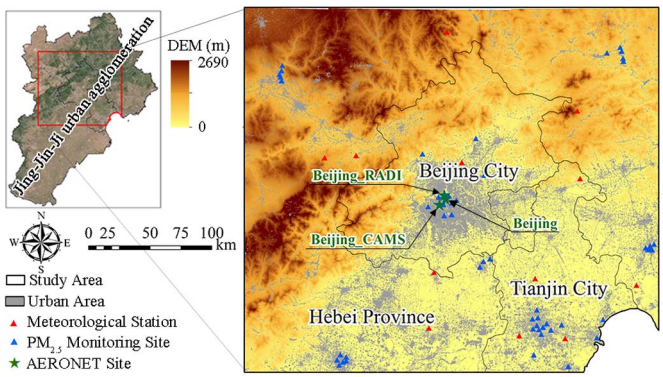

Fig. 1. Study area and locations of $PM_{2.5}$ related monitoring sites.

comprising Beijing City, most of Tianjin City, and parts of Hebei Province. The entire area is 84 376 km^2 and includes 84 189 discrete 1×1 km grid cells (see Fig. 1). Air pollution, particularly $PM_{2.5}$ pollution, is the primary environmental problem in this area due to the continental air masses and high aerosol loadings coming from both local and regional sources.

B. Data and Predictors

In this letter, Aqua-MODIS swath products (MYD02HKM, MYD03, and MYD09), AOD products, Aerosol Robotic Network (AERONET) data, ground-level $PM_{2.5}$ concentrations, and other auxiliary data for 2013 were used. AEORNET level 2.0 AOD measurements from the Beijing site were used to retrieve SARA AODs based on the Aqua-MODIS swath images (MYD02HKM, MYD03, and MYD09), and the retrieved AOD was validated using AERONET level 1.5 from Beijing_RADI and Beijing_CAMS sites. For comparison purpose, the Aqua-MODIS Dark Target Collection (C006) AOD products at 3 km (MYD04_3K) [11] and 10 km (MYD04) resolutions were also obtained. To reduce the negative influence of cloud on the quality of MODIS images and AODs in the study domain, all the AODs were transformed to annual average.

Meanwhile, annual average $PM_{2.5}$ concentrations (μg/m^3) of 52 monitoring stations were also produced based on the hourly observation data from the China National Environmental Monitoring Centre (CNEMC) (http://cnemc.cn). Auxiliary data such as locations of industrials, populations, road networks, land use/covers, and meteorological data were also collected and preprocessed at the annual scale. The meteorological data were downloaded from the China Meteorological Data Service System (http://cdc.cma.gov.cn) which include parameters like temperature (degree), relative humidity (%), and atmospheric pressure (hPa) at 13 monitoring sites.

Furthermore, predictors containing industrial density (number/km^2), population density (person/km^2), main road length (km), area ratio of a certain type of land use (e.g., forest and water) to the total area of an area (%), and dust area percentage (DAP) (%) were developed based on previous research findings [12]. All these predictor values were quantified over a 1-km radius buffer at each $PM_{2.5}$ monitoring site [3], [13]. Values of meteorological predictors (i.e., temperature, relative humidity, and atmospheric pressure) for all the $PM_{2.5}$ monitoring sites were assigned based on the corresponding values of the nearest meteorological station. In this process, we used the "absolute deviation" of temperature instead of the directly observed temperatures. Additionally, these predictors were further screened out to establish effective $PM_{2.5}$ simulation models. This process was implemented by Pearson's correlation analysis between the predictor values and annual $PM_{2.5}$ concentrations. The predictors screened out in this letter are SARA AOD, DAP, and absolute deviation of temperature (DTEMP).

III. Methodology

A. SARA AOD Retrieving

SARA retrieves AOD [see (1)] based on real viewing geometry and wider range of aerosol types and conditions, without using the common technique of constructing a lookup table [14]–[16]. SARA has three assumptions to make AOD retrieval: 1) The land surface is Lambertian; 2) single scattering approximation; and 3) the single scattering albedo (SSA) (ω_0) and asymmetric factor (g) do not vary spatially over the region on the day of retrieval. For SARA, the top of atmosphere (TOA) reflectance is obtained from MYD02HKM, solar and sensor angles (zenith and azimuth) from MYD03, surface reflectance from the MYD09 product [17], and input AOD from the Beijing AERONET site

$$\tau_{a,\lambda}=\frac{4\mu_s\mu_v}{\omega_0 P_\alpha(\theta_s,\theta_v,\varphi)}\Bigg[\rho_{\mathrm{TOA}}(\lambda,\theta_s,\theta_v,\phi)-\rho_{\mathrm{Ray}}(\lambda,\theta_s,\theta_v,\phi) -\frac{e^{-(\tau_R+\tau_{\alpha,\lambda})/\mu_s}e^{-(\tau_R+\tau_{\alpha,\lambda})/\mu_v}\rho_s(\lambda,\theta_s,\theta_v,\phi)}{1-\rho_s(\lambda,\theta_s,\theta_v,\phi)(0.92\tau_R+(1-g)\tau_{\alpha,\lambda})\exp\left[-(\tau_R+\tau_{\alpha,\lambda})\right]}\Bigg] \tag{1}$$

where

$\tau_{a,\lambda}$	AOD
τ_R	Rayleigh optical depth
$\rho_{\mathrm{TOA}}(\lambda,\theta_s,\theta_v,\phi)$	TOA reflectance
$\rho_{\mathrm{Ray}}(\lambda,\theta_s,\theta_v,\phi)$	Rayleigh reflectance
$\rho_s(\lambda,\theta_s,\theta_v,\phi)$	surface reflectance
μ_s	cosine of solar zenith angle
μ_v	cosine of sensor zenith angle
ω_0	SSA
g	asymmetry parameter
$P_\alpha(\theta_s,\theta_v,\phi)$	aerosol phase function.

The validation of SARA AOD is conducted using AERONET level 1.5 AOD data from the Beijing_RADI and Beijing_CAMS sites. Owing to cloud cover, atmospheric spatial variability, and the purpose of increasing the number of statistical samples, the sun photometer AOD from AERONET is averaged within 2 h of the MODIS local overpass time. For details of SARA, interested readers can refer to [14] and [15].

B. GWR Model Structure

As a practical technique extending the ordinary linear regression framework, GWR can examine the spatial variation and

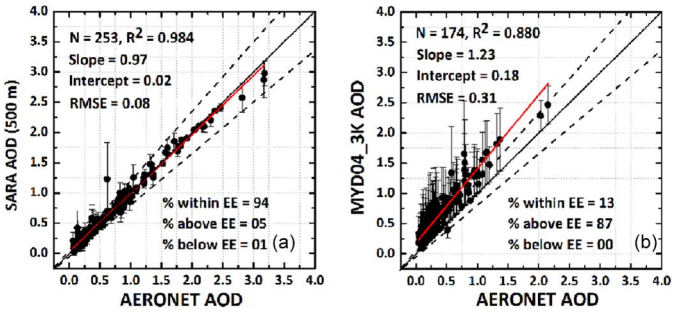

Fig. 2. Validation of SARA-retrieved AOD at 1-km resolution against Beijing_RADI and Beijing_CAMS AERONET AOD measurements.

nonstationarity for continuous surface of parameter values at the regional scale [18]. The general structure of the GWR model developed in this letter is as follows:

$$\mathrm{PM}_{2.5,s} = \beta_{0,s} + \beta_{1,s}\mathrm{AOD}_s + \beta_{2,s}\mathrm{DTEMP}_s + \beta_{3,s}\mathrm{DAP}_s + \varepsilon_s \tag{2}$$

where s is the unique Identify number of $\mathrm{PM}_{2.5}$ monitoring sites, $\mathrm{PM}_{2.5,s}$ is the estimation of annual average $\mathrm{PM}_{2.5}$ concentration serving as the dependent variables of a site s, and AOD_s, DTEMP_s, and DAP_s are independent variables. $\beta_{0,s}$ indicates the intercept of the GWR model, $\beta_{1,s} - \beta_{e,s}$ are coefficients describing the unique spatial relationship between dependent and independent variables around site s, and ε_s is the error term.

Since a set of one or more geographically independent variables would be measured at their spatial locations in GWR models, values of a dependent variable can be estimated anywhere across the study area by using geographical weighting. The nature of the geographical weighting coefficients for each location can be described as

$$\hat{\beta}(s) = \left(X^T W(s) X\right)^{-1} X^T W(s) y \tag{3}$$

where $X^T W(s) X$ represents the geographically weighted variance–covariance matrix and y is a vector containing values of the dependent variable. $W(s)$ is the square matrix of the weight matrix that carries 0 in its off-diagonal elements and the geographical weights in its leading diagonal, which are computed through a weighting scheme known as a kernel function

$$w_i(s) = e^{-0.5\left(\frac{d_i(s)}{h}\right)^2} \tag{4}$$

where $w_i(s)$ is the geographical weight of the ith observation relative to the location s in the data set, $d_i(s)$ is the distance between the ith observation and the location s, and h represents the bandwidth. The unit of bandwidth in the kernel function is the same to those from location coordinates. The weights will approach unity with growing bandwidths and consequently promote the transformations of local GWR models into the global OLS model. The finalized GWR model is generally ascertained based on the model performance denoted by fitting the R^2 (highest) and the $\mathrm{AIC_c}$ (lowest) value.

TABLE I
PARAMETERIZATION AND MODEL FITTING OF GWR AND OLS MODELS

Statistical models	OLS		GWR	
	Predictors	Coefficient	Variables	Value
Model fitting				
	SARA AOD	44.634	B	80000.000
	TEMP	-12.840	AICc	427.593
	DSP	0.072	EN	13.628
	Constant	78.451	Sigma	12.482
			RS	5978.404

B, EN, and RS represent bandwidth, effective number, and residual squares, respectively.

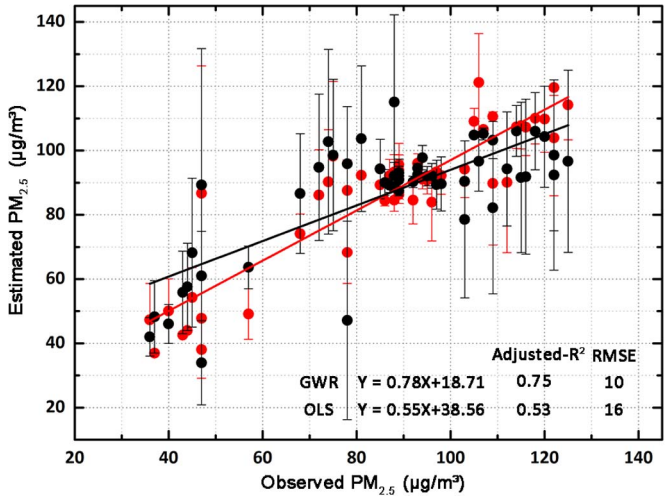

Fig. 3. Validation of annual mean $\mathrm{PM}_{2.5}$ concentrations predicted by the GWR and OLS models with ground-level $\mathrm{PM}_{2.5}$ measurements over 52 sites.

C. OLS Model Structure

While the values of coefficient $\beta_{k,s}$ of dependent variables in the GWR model are not geographically varied within the study domain, the regression model under that situation is actually an OLS model with spatial homogeneity [19]

$$\mathrm{PM}_{2.5,s} = \beta_0 + \beta_1 \mathrm{AOD}_s + \beta_2 \mathrm{DTEMP}_s + \beta_3 \mathrm{DAP}_s + \varepsilon \tag{5}$$

where β_k $(k = 0, 1, 2, 3)$ are the regression coefficients estimated under a condition that the value of $\sum_{i=1}^{s}(y_i - \hat{y}_i)^2$ is minimized over the observations. In this letter, the OLS mode is designed to comparatively validate the performance of the GWR model in mapping $\mathrm{PM}_{2.5}$ concentration distribution.

D. $PM_{2.5}$ Concentration Mapping

To produce the continuous $\mathrm{PM}_{2.5}$ concentration surface using the GWR and OLS models, a 1-km resolution fishnet covering the entire study area is first created. Then, values of the modeling predictors (i.e., dependent variables AODs, DTEMP, and DAP) at the corner locations of this fishnet are measured using the methods stated in the "Data and Predictors" section. Meanwhile, values of geographically varied coefficients of dependent variables at these corner locations are also interpolated by ordinary Kriging based on the values at the monitoring sites ascertained in the GWR model construction process. Finally,

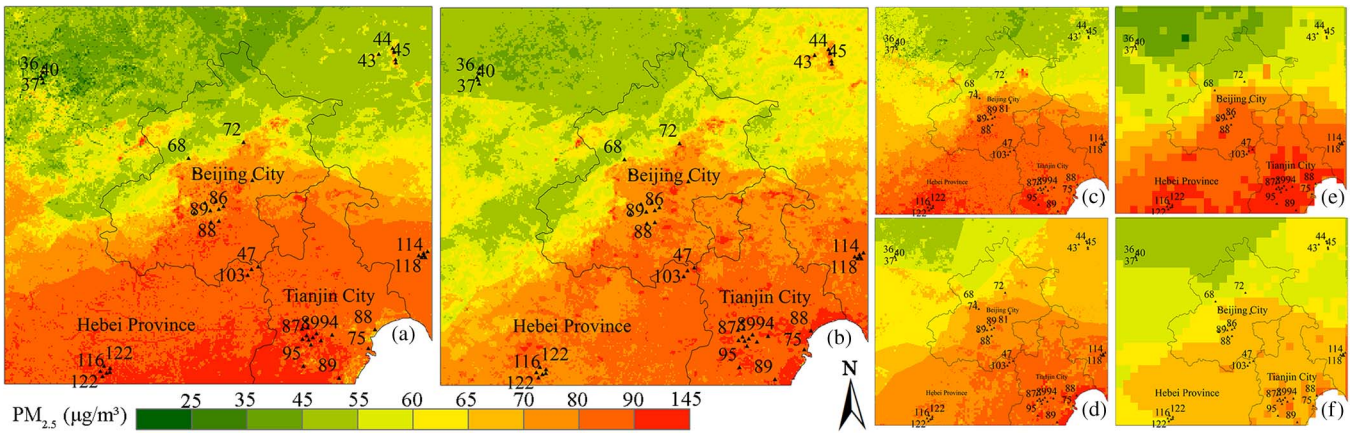

Fig. 4. Spatial distribution of annual mean $PM_{2.5}$ concentrations estimated by (a) GWR and (b) OLS models by using SARA AOD at 1 km, compared to those MYD04_3K AOD at 3 km (i.e., (c) GWR and (d) OLS) and MYD04 AOD at 10 km (i.e., (e) GWR and (f) OLS).

we calculated the $PM_{2.5}$ concentrations at all the cross-locations of the preset fishnet using the algebraic equation [see (2) and (5)] of the GWR and OLS models and yielded grid level $PM_{2.5}$ concentration estimates at resolutions of 1, 3, and 10 km (for reference), respectively.

E. Model Validation

Cross-validation (CV) is a widely used method to evaluate the performance of models that usually have limited data samples [9]. Thus, tenfold CV is further developed for validating the performance stability of the GWR and OLS models in this letter by randomly taking out the data at 90% of modeling sites as the training set, with the remaining 10% as the test set. In this process, the root-mean-squared error (*RMSE*), standard deviation (*SD*), and mean relative tolerance (*MRT*) between the estimated $PM_{2.5}$ concentrations and remaining observed ones are employed as the validation statistics.

IV. Results and Discussion

Validations of SARA AOD and MODIS AOD were conducted using ground-level AOD measurements from the Beijing_RADI and Beijing_CAMS AERONET sites (see Fig. 2). The red solid and dotted lines represent the regression and confidence-envelope-of-expected-error line, respectively. SARA provides almost 45% more data points than MOD04_3K, and a better agreement between SARA AOD and AERONET AOD is observed with significant overall correlations (R) of 0.984. A higher scattering is observed at low AOD values for MOD04_3K, while SARA maintains prominent AOD accuracy (*RMSE* 0.08-SARA over 0.31-MOD04_3K). Hence, SARA can generate superior quality-assured AOD data.

Table I and Fig. 3 summarize the parameters of the fitted GWR and OLS models based on SARA AOD at 1-km resolution. The overall mean adjusted $R^2 = 0.75$ of the GWR model is greater than that of the OLS (i.e., R^2: 0.53) which confirms the superiority of the GWR model to the OLS model in simulating site-based $PM_{2.5}$ concentrations. The result also demonstrates that the estimated $PM_{2.5}$ concentrations from both models have a good agreement with the observed ones ranging from 85 to 100 $\mu g/m^3$. However, the OLS model is prone to be underestimated at high concentration levels (105–145 $\mu g/m^3$) and overestimated at medium concentration levels (50–80 $\mu g/m^3$) when compared with the GWR model. This finding also indicates that more local sublinearity between fine-scale AOD and $PM_{2.5}$ concentrations in a wide geographic area perhaps can be better interpreted by the GWR model. Moreover, these results are echoed by the *RMSEs* for the GWR model (10 $\mu g/m^3$) and the OLS model (16 $\mu g/m^3$).

Fig. 4 illustrates the spatially continuous surface of the estimated $PM_{2.5}$ concentrations (annual mean). Apparently, the $PM_{2.5}$ concentrations in almost all of the study area exceeded the Level 2 standard of the Chinese National Ambient Air Quality Standard (35 $\mu g/m^3$) in 2013 [20]; obviously, spatial heterogeneity still occurred. The high-level $PM_{2.5}$ concentrations $(> 65\ \mu g/m^3)$ are clustered in the centered urban and commercial districts due to the surrounding industries, traffic emission sources, and surface dusts in the prevailing wind direction. Contrarily, low concentration $(< 25\ \mu g/m^3)$ mainly appears in the rural or mountain areas as expected, such as in Changping, Chengde, Taihang mountain, and the northern half and western part of the study area.

Comparison of Fig. 4(a) and (b) demonstrates that higher concentrations of $PM_{2.5}$ in the southwestern part of the study domain (e.g., Baoding City) estimated by the GWR model matched better with the corresponding ground-level measurement than those from the OLS model, while it remains the same for lower estimates. These results further suggest that the GWR model can significantly outperform the OLS model in continuously revealing the spatial variability of $PM_{2.5}$ concentration over large geographic area. Moreover, differences of the spatial distributions of $PM_{2.5}$ estimates in Fig. 4(a)–(f) disclose that models based on AOD at 1- and 3-km resolutions [see Fig. 4(a)–(d)] can yield much finer spatial details than the one at 10-km resolution [see Fig. 4(e) and (f)]. The spatial distributions of $PM_{2.5}$ concentrations estimated by the GWR and OLS models using SARA AOD at 1-km resolution are

TABLE II
TENFOLD CV OF GWR AND OLS MODELS (μg/m^3)

CV	GWR 1 km	GWR 3 km	GWR 10 km	OLS 1 km	OLS 3 km	OLS 10 km
SD	10	11	19	16	18	25
RMSE	11	11	19	16	17	25
MRT	10.47%	10.47%	16.58%	16.99%	16.92%	21.37%

correlated better with ground-level $PM_{2.5}$ measurements than those using MOD04 AOD at 3- and 10-km resolutions. Moreover, these differences are much more sensitive for the GWR model relative to the OLS model at 10-km resolution, revealing that both GWR and OLS models could be plagued with spatial resolution.

Additionally, results of the tenfold CV in Table II echoed Fig. 4 that the GWR model can obviously improve the estimation accuracy of $PM_{2.5}$ concentrations relative to the OLS model. The *SD*, *CVRMSE*, and *MRT* of the GWR (SARA) model are 11 μg/m^3, 11 μg/m, and 10.47%, respectively, while those from the OLS model are 16 μg/m^3, 16 μg/m^3, and 16.99%. Models based on MODIS AOD at 3 km yield similar CV results as that at 10 km, but significantly with higher errors. Relative greater variation ratios of these statistics indicate that the GWR model is more sensitive to the spatial variations of predictors over a large geographic region and can always generate relatively more accurate estimates than the OLS model. High-resolution AOD is much more essential for accurate $PM_{2.5}$ estimation in GWR modeling than in OLS.

V. CONCLUSION

Sparse ground-level monitoring and uncertain satellite-based AOD generally impeded the fine-scale mapping of $PM_{2.5}$ concentration in urban area due to the inherent defects of the traditional AOD retrieval algorithm and spatial nonstationary relationship between $PM_{2.5}$ and AOD. In this letter, SARA-retrieved AOD at 1-km resolution is utilized to estimate $PM_{2.5}$ concentrations over the Jing-Jin-Ji urban agglomeration which suffers from the most heavy air pollution in China. The main purpose of this letter is to test the combination of high-resolution AOD and GWR technique, whether it can promote or not the capacity of finely distinguishing spatial patterns of $PM_{2.5}$ concentration levels. The GWR and OLS models are established with the SARA AOD at 1-km resolution as a major predictor, and the performances of these two models are compared based on MOD04 AOD at 3- and 10-km resolutions to investigate the advantages of this combination scheme.

Importantly, the satellite-based GWR statistics with the acceptable adjusted fitting R^2 and *RMSE* shows significant improvements in $PM_{2.5}$ estimation and in spatial pattern depiction when compared with the OLS statistics. These comparable findings relative to previous studies [9], [12], [19] strongly confirmed the feasibility and reliability of the usage of the combination of high-resolution AOD and GWR technique to refine the $PM_{2.5}$ map in urban area, and this will also be helpful for the remote-sensing-based monitoring site selection and refinement of air pollution control strategies.

ACKNOWLEDGMENT

The authors would like to thank the National Aeronautics and Space Administration Goddard Space Flight Center for the MODIS sensor data. The authors would also like to thank the China Meteorological Administration for providing the climate data.

REFERENCES

[1] B. Zou, J. G. Wilson, F. B. Zhan, and Y. Zeng, "Air pollution exposure assessment methods utilized in epidemiological studies," *J. Environ. Monit.*, vol. 11, no. 3, pp. 475–490, Mar. 2009.
[2] C. Lin *et al.*, "Using satellite remote sensing data to estimate the high-resolution distribution of ground-level $PM_{2.5}$," *Remote Sens. Environ.*, vol. 156, pp. 117–128, Jan. 2015.
[3] B. Zou *et al.*, "Spatial modeling of $PM_{2.5}$ concentrations with a multifactoral radial basis function neural network," *Environ. Sci. Pollut. Res.*, vol. 22, no. 14, pp. 10 395–10 404, Jul. 2015.
[4] J. Wang and S. A. Christopher, "Intercomparison between satellite-derived aerosol optical thickness and $PM_{2.5}$ mass: Implications for air quality studies," *Geophys. Res. Lett.*, vol. 30, no. 21, pp. 1–4, Nov. 2003.
[5] B. Zou, Y. Guo, Y. Q. Tang, S. Xu, and Q. H. Weng, "Remote sensing detection of the spatial pattern of urban air pollution in Los Angeles," in *Proc. IEEE EORSA*, 2014, pp. 251–255.
[6] W. Z. Song, H. F. Jia, J. F. Huang, and Y. Y. Zhang, "A satellite-based geographically weighted regression model for regional $PM_{2.5}$ estimation over the Pearl River Delta region in China," *Remote Sens. Environ.*, vol. 154, pp. 1–7, Nov. 2014.
[7] A. A. Kokhanovsky *et al.*, "Aerosol remote sensing over land: A comparison of satellite retrievals using different algorithms and instruments," *Atmos. Res.*, vol. 85, no. 3/4, pp. 372–394, Sep. 2007.
[8] M. S. Wong, J. E. Nichol, and K. H. Lee, "An operational MODIS aerosol retrieval algorithm at high spatial resolution, and its application over a complex urban region," *Atmos. Res.*, vol. 99, no. 3/4, pp. 579–589, Mar. 2011.
[9] Z. W. Ma, X. F. Hu, L. Huang, J. Bi, and Y. Liu, "Estimating ground-level $PM_{2.5}$ in China using satellite remote sensing," *Environ. Sci. Technol.*, vol. 48, no. 13, pp. 7436–7444, Jun. 2014.
[10] X. Hu *et al.*, "Estimating ground-level $PM_{2.5}$ concentrations in the southeastern US using geographically weighted regression," *Environ. Res.*, vol. 121, pp. 1–10, Feb. 2013.
[11] L. A. Remer, S. Matto, R. C. Levy, and L. Munchak, "MODIS 3 km aerosol product: Algorithm and global perspective," *Atmos. Meas. Tech.*, vol. 6, no. 7, pp. 1829–1844, Jul. 2013.
[12] I. Kloog, F. Nordio, B. A. Coull, and J. Schwartz, "Incorporating local land use regression and satellite aerosol optical depth in a hybrid model of spatiotemporal $PM_{2.5}$ exposures in the Mid-Atlantic states," *Environ. Sci. Technol.*, vol. 46, no. 21, pp. 11 913–11 921, Sep. 2012.
[13] B. Zou *et al.*, "Performance comparison of LUR and OK in $PM_{2.5}$ concentration mapping: A multidimensional perspective," *Sci. Rep.*, vol. 5, no. 8698, pp. 1–7, Mar. 2015.
[14] M. Bilal, J. E. Nichol, M. P. Bleiweiss, and D. Dubois, "A simplified high resolution MODIS aerosol retrieval algorithm (SARA) for use over mixed surfaces," *Remote Sens. Environ.*, vol. 136, pp. 135–145, Sep. 2013.
[15] M. Bilal, J. E. Nichol, and P. W. Chan, "Validation and accuracy assessment of a Simplified Aerosol Retrieval Algorithm (SARA) over Beijing under low and high aerosol loadings and dust storms," *Remote Sens. Environ.*, vol. 153, pp. 50–60, Oct. 2014.
[16] M. Bilal and J. E. Nichol, "Evaluation of MODIS aerosol retrieval algorithms over the Beijing-Tianjin-Hebei region during low to very high pollution events," *J. Geophys. Res. Atmos.*, vol. 120, no. 15, pp. 7941–7957, Aug. 2015.
[17] M. Nazeer, J. E. Nichol, and Y. K. Yung, "Evaluation of atmospheric correction models and Landsat surface reflectance product in an urban coastal environment," *Int. J. Remote Sens.*, vol. 35, no. 16, pp. 6271–6291, Aug. 2014.
[18] C. Brunsdon, A. S. Fotheringham, and M. E. Charlton, "Geographically weighted regression: A method for exploring spatial nonstationarity," *Geographical Anal.*, vol. 28, no. 4, pp. 281–298, Oct. 1996.
[19] Y. Liu, C. J. Paciorek, and P. Koutrakis, "Estimating regional spatial and temporal variability of PM concentrations using satellite data, meteorology, and land use information," *Environ. Health Perspectives*, vol. 117, no. 6, pp. 886–892, Jun. 2009.
[20] China National Air Quality Standards, GB 3095-2012, 2013. [Online]. Available: http://chinacsrmap.org/CSRTool_Show_EN.asp?ID=285